diversity

MDPI

Article

Plastomes Provide Insights into Differences between Morphology and Molecular Phylogeny: *Ostericum* and *Angelica* (Apiaceae) as an Example

Qiu-Ping Jiang, Chang-Kun Liu, Deng-Feng Xie, Song-Dong Zhou and Xing-Jin He *

Key Laboratory of Bio-Resources and Eco-Environment of Ministry of Education, College of Life Sciences, Sichuan University, Chengdu 610065, China
* Correspondence: xjhe@scu.edu.cn

Abstract: Traditional classification based on morphological characters suggests that the genus *Ostericum* is closely related to *Angelica*, but molecular phylogenetic studies suggest that the genus *Ostericum* is related to *Pternopetalum* rather than *Angelica*. In this study, the plastomes of nine *Ostericum* species and five *Angelica* species were used to conduct bioinformatic and comparative analyses. The plastomes of *Ostericum* and *Angelica* exhibited significant differences in genome size, gene numbers, IR junctions, nucleotide diversity, divergent regions, and the repeat units of SSR types. In contrast, *Ostericum* is more similar to *Pternopetalum* rather than *Angelica* in comparative genomics analyses. In total, 80 protein-coding genes from 97 complete plastomes and 112 ITS sequences were used to reconstruct phylogenetic trees. Phylogenies showed that *Angelica* was mainly located in Selineae tribe while *Ostericum* was a sister to *Pternopetalum* and occurred in the *Acronema* clade. However, morphological analysis was inconsistent with molecular phylogenetic analysis: *Angelica* and *Ostericum* have similar fruit morphological characteristics while the fruits of *Ostericum* are quite different from the genus *Pternopetalum*. The phylogenetic relationship between *Angelica* and *Ostericum* is consistent with the results of plastome comparisons but discordant with morphological characters. The cause of this phenomenon may be convergent morphology and incomplete lineage sorting (ILS).

Keywords: *Angelica*; *Ostericum*; comparisons; morphological; phylogenetic; plastomes

check for updates

Citation: Jiang, Q.-P.; Liu, C.-K.; Xie, D.-F.; Zhou, S.-D.; He, X.-J. Plastomes Provide Insights into Differences between Morphology and Molecular Phylogeny: *Ostericum* and *Angelica* (Apiaceae) as an Example. *Diversity* **2022**, *14*, 776. https://doi.org/10.3390/d14090776

Academic Editor: Michael Wink

Received: 12 August 2022
Accepted: 14 September 2022
Published: 19 September 2022

1. Introduction

The division of species and the evolutionary relationship between them are the basis of biology. Over the last 50 years, phylogeny has become increasingly more based on molecular data, increasingly favoring homologous sequences rather than morphological characters [1]. Molecular phylogeny had been widely used to evaluate traditional plant taxonomy (e.g., Angiosperm Phylogeny Group III and IV (APG III, 2009; APG IV, 2016)) [2,3]. The differences between morphology and molecular phylogeny come under observation in many plants. For example, the phylogeny based on molecular data of *Hedyosmum* (Chloranthaceae) indicated differences between morphology and molecular phylogeny [4], and similar circumstances have been found among Restionaceae, Anarthriaceae, and Centrolepidaceae [2,5]. In addition, this phenomenon is very common in Apiaceae, especially in Apioideae. The Apioideae were divided into 8 tribes and 10 subtribes based on fruit morphology, but a total of 41 major clades within Apioideae have been identified based on molecular phylogenetic studies [6–8].

Apioideae is the largest and best-known subfamily of Apiaceae and includes many familiar edible and medicinal plants in China (e.g., *Daucus carota* var. *sativa* Hoffm., *Coriandrum sativum* L., *Peucedanum praeruptorum* Dunn, *Bupleurum chinense* DC.) [7,9,10]. The species of Apioideae are difficult to attribute to known genera and species. Most traditional classifications of Apiaceae have relied almost exclusively on fruit characters [11]. However, major classifications of Apioideae produced some differences between morphology and

molecular phylogeny [8,12–14]. A typical example is that *Angelica* L. is consistent with *Ostericum* Hoffm. in the morphological characteristics (e.g., fruits (Figure 1), flowers, and leaves) but distantly related to *Ostericum* in molecular phylogenetic studies [8,15,16].

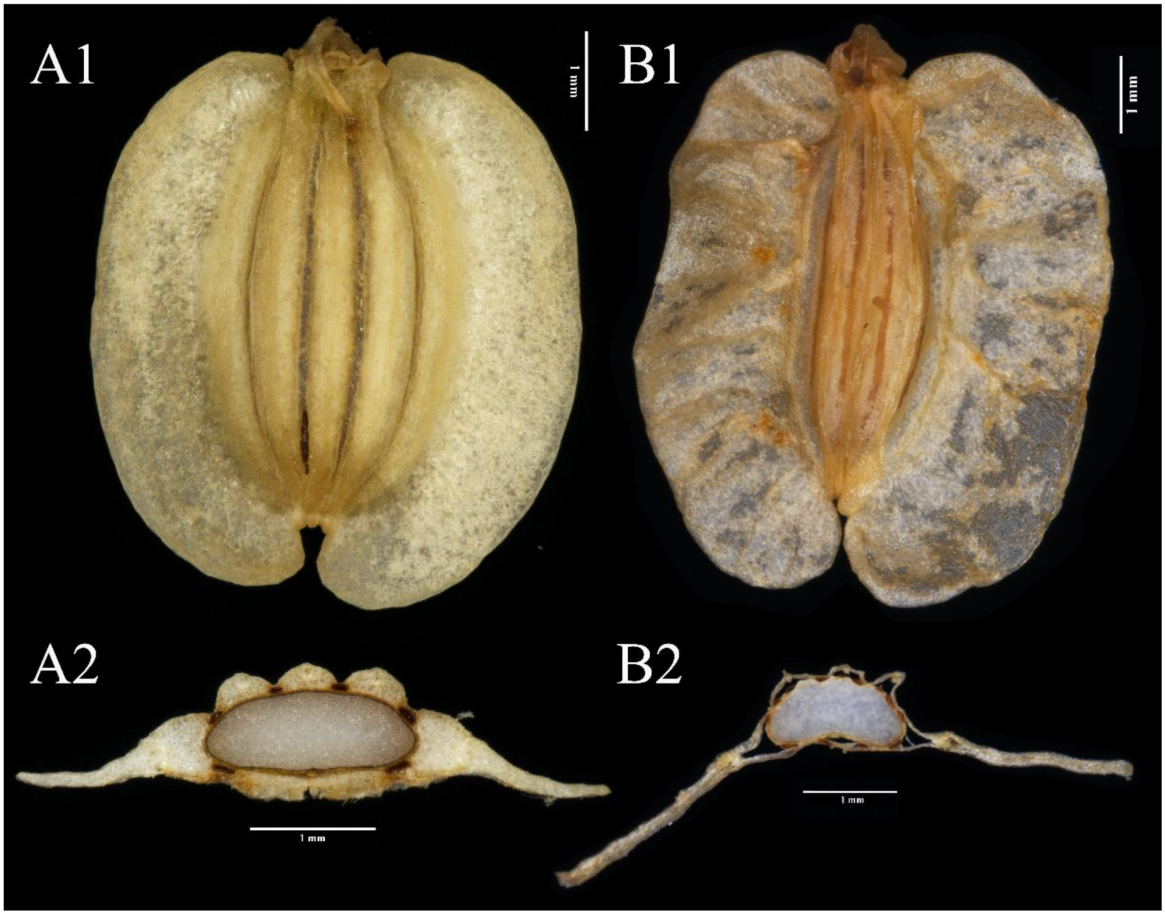

Figure 1. Fruit of (**A**) *Angelica dahurica*; (**B**) *Ostericum scaberulum*. (**A1**,**B1**) Dorsal view of fruit; (**A2**,**B2**) Cross-section of fruit.

Angelica is a large and taxonomically complex genus of Apiaceae that comprises more than approximately 100 species around the world [9,10,17,18]. The genus *Angelica* with related genera, including *Archangelica* Wolf, *Coelopleurum* Ledeb., *Conioselinum* Fisch. ex Hoffm., *Czernaevia* Turcz., *Glehnia* F. Schmidt ex Miq., *Levisticum* Hill, and *Ostericum*, is composed of a large and controversial group called Angelicinae Drude in *Flora Reipublicae Popularis Sinicae* [9] or *Angelica* sensu lato in some other publications [19]. This group is widely distributed in northern temperate regions and exhibits high diversities and variations in morphology, resulting in problematic generic limits [9,10]. In addition, there are many economically important plants in *Angelica* and *Ostericum*. Among them, *A. dahurica* (Fisch. ex Hoffm.) Benth. et Hook. f. ex Franch. e, *A. decursiva* (Miquel) Franchet & Savatier, and *O. citriodorum* (Hance) Yuan et Shan are commonly used as traditional Chinese medicines [9,10]; *A. amurensis* Schischk. Is used as food or fodder for animals; and *O. grosseserratum* (Maxim.) Kitagawa and *O. maximowiczii* (Fr. Schmidt ex Maxim.) Kitagawa can also be used to extract aromatic oils [9,10]. An in-depth study of the two genera will undoubtedly provide new basic information on the origin and species evolution and improve the resource utilization of these genera.

Ostericum was first described by Hoffmann, with *O. palustre* (Besser) Besser as the type species. The genus is mainly distributed in the north temperate zone, containing approximately 13 species worldwide, with 11 species distributed in China [9,10,17,20]. Since the establishment of the genus *Ostericum*, the taxonomic position of this genus has

been controversial. Maximowicz (1873) moved *Ostericum* into *Angelica* as an infrageneric section [21]. Drude (1898), based on fruit morphology, incorporated *Ostericum* and eight other genera into *Angelica*, and *Ostericum* became a subgenus named subgen. *Ostericum* Maxim [11]. In contrast, other botanists suggested that *Ostericum* should be independent of *Angelica*. Kitagawa suggested that *Ostericum* should be treated as a relatively independent genus based on fruit morphological studies in 1935 [22]. Through chemical composition analysis, Harborne held the same opinion [23]. Additionally, after study of the fruit anatomy and pollen ultrastructure of *Angelica* L. (S. L.), Qin et al. (1995) and Sheh et al. (1997) [24–26] regarded *Ostericum* as an independent genus and the controversy was also embodied in the *flora* of different regions. In the *Umbelliferae of Japan* and *North American Flora*, *Ostericum* was moved into *Angelica* [19,27]. In *Flora Reipublicae Popularis Sinicae* and *Flora of China*, *Ostericum* was treated as an independent genus but was still considered to be closely related to *Angelica* [9,10].

With the development of DNA sequencing technology, several molecular markers, such as nuclear DNA (nrDNA), including internal transcribed spacer (ITS) sequences and external transcribed spacer (ETS), and the plastid fragments (rpl16 and rps16), have been used to infer the phylogeny of Apioideae [6–8,28–31]. The same is true for the genus *Ostericum* and *Angelica*, as molecular phylogenetic analysis showed that *Ostericum* and *Angelica* had distant relationships based on ITS, ETS, and plastid fragments [8,15,16], except for *O. huadongensis* Z. H. Pan & X. H. Li, which inserted into *Angelica* in Liao et al.'s (2013) study [16]. These studies' main target species was the genus *Angelica*, which contains few species of *Ostericum*, and does not contain the type species of *Ostericum* (*O. palustre*). The plastid DNA has many features, such as monolepsis, small subfractions, multiple replications, and moderate nucleotide substitution rates. Because of these specific features, and with an increasing number of plastomes available from the National Center for Biotechnology Information (NCBI), plastomes have been widely used for the reconstruction of phylogenetic relationships at different taxonomic ranks in angiosperms [32–36]. Moreover, plastomes have been exploited in molecular identification, comparative genomics, genome evolution, and population genetics [37–40].

To date, many complete plastomes of Apiaceae species have been published, including some species of *Angelica* and *Ostericum* [41–43]. In this study, we sequenced and annotated the plastomes of five species of *Angelica* and eight species of *Ostericum*, combined with the plastome of *O. palustre* (obtained from NCBI). We aimed to (1) explore the possible causes of differences in molecular phylogenetic and morphological studies between *Angelica* and *Ostericum*; (2) perform comparative analysis of plastomes to provide insights into differences between morphology and molecular phylogeny; and (3) reconstruct phylogenetic relationships of *Ostericum* based on complete plastomes. The scientific names and abbreviations of the species involved in this study are listed in Supplementary Material Table S1.

2. Materials and Methods

2.1. Taxon Sampling, DNA Extraction, and Sequencing

Fresh leaves were collected from wild plants, and they were desiccated and stored in silica gel. We extracted the total genomic DNA from the stored dry leaves using a modified cetyltrimethylammonium bromide method [44]. The herbarium specimens of these species were stored in the Herbarium, College of Life Sciences, Sichuan University (SZ). The specimen voucher details are shown in Table S2. These plants are not key protected plants and the collection of plant material complied with institutional or national guidelines and was conducted following local legislation.

For nrITS, PCR amplification of the complete ITS region used the primers of ITS4 (5′-TCC TCCGCT TAT TGA TAT GC-3′) and ITS5(5′-GGA AGTAAA AGT CGT AAC AAG G-3′) [45]. PCR amplification proceeded in a 30 μL volume reaction, containing 3 μL of plant total DNA, 1.5 μL of each forward primer and reverse primer, 10 μL of ddH_2O, and 15 μL of 2 × Taq MasterMix (CWBIO, Beijing, China). PCR amplification of the nrITS region was

performed under the setting of initial denaturation for 4 min at 94 °C, followed by 30 cycles of 45 s at 94 °C, 45 s at 53 °C, and 60 s at 72 °C, and then the final extension of 10 min at 72 °C. All PCR products were sent to Sangon (Shanghai, China) for sequencing (single-pass sequencing for ITS4 primer) after being examined using a 1.5% (*w*/*v*) agarose TAE gel. The DNA sequences of nrITS were applied for phylogenetic analysis and detailed information is shown in Table S2. For the plastome, these total genomic DNA were sequenced using the Illumina Novaseq-PE1500 platform at Novogene (Beijing, China), with paired-end reads of 2 × 150 bp.

2.2. Plastome Assembly and Annotation

The clean data were assembled using NOVOPlasty 2.7.1 [46] with the default K-mer value of 39 and rbcL of *A. sylvestris* Linnaeus (GenBank accession No. DQ133798.1) was used as seed input for *Angelica* species and rbcL of *O. sieboldii* (Miq.) Nakai (GenBank accession No.: D44579.1) was used as seed input for *Ostericum* species. Preliminary genome annotation was conducted using PGA [47] and manual modifications for uncertain genes, and uncertain start and stop codons were corrected based on comparison with other related plastomes using Geneious R11 [48]. To agree on the standard and reduce error, all the plastomes obtained from NCBI (National Center for Biotechnology Information) were reannotated. Protein-coding gene extraction was performed by PhyloSuite [49]. The sequenced species' annotated genome sequences were submitted to GenBank, and their corresponding accession numbers are listed in Table S2. Circular gene maps of the annotated genomes were constructed using the online program Chloroplot (https://irscope.shinyapps.io/chloroplot/; accessed on 19 May 2022) [50].

2.3. Plastome Comparative Analyses

The junctions between single-copy regions (LSC region and SSC region) and inverted repeat regions (IRA region and IRB region) among these species (we sequenced five species of *Angelica*, eight species of *Ostericum*, and the plastome sequences of *O. palustre* and two species of *Pternopetalum* Franch., which were obtained from NCBI) were compared using Geneious R11 and then visualized manually.

The plastome simple sequence repeats (SSRs) of these species were generated using Perl script MISA [51] with the same settings: 10 repeats for mononucleotide, 5 repeats for dinucleotide, 4 repeats for trinucleotide, 3 repeats for tetranucleotide, 3 repeats for pentanucleotide, and 3 repeats for hexanucleotide.

To compare the plastomes' difference in sequences at the level of the genome, the whole plastomes' alignment of five species of *Angelica*, nine species of *Ostericum*, and *P. davidii* Franch. were generated and visualized using the mVISTA program with the Shuffle-LAGAN model [52], with *P. vulgare* (Dunn) Hand.-Mazz. as the reference. We trimmed the sequences at the *ycf1* gene promoter in IRA region, keeping all sequences of LSC region, IRB region and SSC region.

To detect the nucleotide diversity of plastomes, single nucleotide polymorphism (SNP) analyses were generated using DnaSP v5 [53]. The parameters were set as follows: the window length was 600 bp and the step size was 200 bp. The plastome sequences were aligned using MAFFT v7.402 [54] and calibrated manually in Geneious R11. To minimize the impact of sequences on the plastomes, the alignments of five *Angelica* species and nine *Ostericum* species were trimmed from the *trnH-GUG* gene terminator to the *ycf1* gene promoter manually.

2.4. Phylogenetic Analyses

To infer the phylogenetic relationships between *Angelica* and *Ostericum*, 80 protein-coding genes from 97 complete plastomes and 112 ITS sequences were used to reconstruct phylogenetic trees based on the Bayesian inference (BI) and maximum likelihood (ML) methods. *Chamaesium* H. Wolff was chosen as the outgroup based on previous studies [14]. The protein-coding genes (CDS) were extracted from plastomes using the PhyloSuite

program [49] and with manual checks. The best-fit model was chosen using Modeltest 3.7 [55]. The best-fit model for ITS was GTR+G (BI and ML) and for cpDNA (CDS) was GTR+G (ML) and GTR+G+I (BI), respectively. Maximum likelihood (ML) analyses were undertaken using RAxML v8.2.4 [56] with 1000 bootstrap replicates. Bayesian inference (BI) analyses were performed in MrBayes version 3.2 [57] using a Markov chain Monte Carlo (MCMC) method. We set the number of generations to 10 million starting from a random tree and sampling one tree every 1000 generations. All runs were inspected to check that the average standard deviation of split frequencies was <0.1. The first 20% of the obtained trees were discarded as burn-in and the remaining trees were used to calculate the 50% majority-rule consensus topology and posterior probability (PP) values. The tree display and annotation were performed using the iTOL (https://itol.embl.de/; accessed on 19 May 2022) online tool [58]. In addition, we used the MEGA6 [59] program to detect the characteristics of the CDS data sets and ITS data sets for phylogenetic analysis.

3. Results

3.1. The Plastome Features of Angelica and Ostericum

All complete plastomes of *Angelica* and *Ostericum* had a single and typical quadripartite structure (Figure 2) that was divided into four regions: two inverted repeat regions (IRs), a large single-copy region (LSC), and a small single-copy region (SSC). The size of the plastomes of *Angelica* ranged from 146,765 (*A. biserrata* (Shan et Yuan) Yuan et Shan) to 147,308 bp (*A. tianmuensis* Z. H. Pan & T. D. Zhuang) and that of *Ostericum* ranged from 154,923 (*O. palustre*) to 160,904 bp (*O. atropurpureum* G.Y.Li, G.H.Xia & W.Y.Xie). The IR regions ranged from 17,817–18,217 bp in *Angelica* and ranged from 25,224–26,443 bp in *Ostericum*, the small single-copy regions (SSC) ranged from 17,504–17,674 bp in *Angelica* and from 17,436–23,685 bp in *Ostericum*, and the large single-copy regions (LSC) ranged from 93,201–93,539 bp in *Angelica* and from 84,686–90,625 bp in *Ostericum*. The genome total GC content was 37.5% in *Angelica* and 37.4–37.7% in *Ostericum*. The plastomes of the *Angelica* and *Ostericum* shared 114 unique genes, including 80 protein-coding genes (PCGs), 30 transfer RNA genes (tRNAs), and 4 ribosomal RNA genes (rRNAs). The total number of genes in *Angelica* was 129 while in *Ostericum*, it was 134. The total number of protein-coding genes (PCGs) in *Angelica* was 84 while in *Ostericum*, it was 87. The total number of transfer RNA genes (tRNAs) in *Angelica* was 36 while in *Ostericum*, it was 37. Compared to *Angelica*, *Ostericum* had four more duplicated genes: *trnI-CAU*, *ycf2*, *rpl23*, and *rpl2* (Tables 1 and 2). The amount of genes, PCGs, tRNAs, and rRNAs of *Pternopetalum* was identical to *Ostericum*. Additionally, the size of *Pternopetalum* plastomes, LSC length, SSC length, and IR length were similar to *Ostericum* (Table 1).

Table 1. Features of the plastid genomes of *Angelica*, *Ostericum*, and *Pternopetalum* species.

Species	Size (bp)	LSC Length (bp)	SSC Length (bp)	IR Length (bp)	Number of Different Genes/Total Number of Genes	Number of Different Protein-Coding Genes (Duplicated in IR)	Number of Different tRNA Genes (Duplicated in IR)	Number of Different rRNA Genes (Duplicated in IR)	Number of Genes Duplicated in IR	GC Content (%)
A. sylvestris	147,138	93,459	17,563	18,058	114/129	80 (4)	30 (6)	4 (4)	15	37.5
A. amurensis	146,931	93,201	17,558	18,086	114/129	80 (4)	30 (6)	4 (4)	15	37.5
A. biserrata	146,765	93,297	17,504	17,982	114/129	80 (4)	30 (6)	4 (4)	15	37.5
A. dahurica	146,847	93,539	17,674	17,817	114/129	80 (4)	30 (6)	4 (4)	15	37.5
A. tianmuensis	147,308	93,238	17,636	18,217	114/129	80 (4)	30 (6)	4 (4)	15	37.5
O. palustre	154,923	84,686	17,699	26,274 (26,264)	114/134	80 (7)	30 (7)	4 (4)	20	37.5
O. atropurpureum	160,904	90,625	17,521	26,379	114/134	80 (7)	30 (7)	4 (4)	20	37.7
O. citriodorum	155,883	85,319	19,722	25,421	114/134	80 (7)	30 (7)	4 (4)	20	37.6
O. grosseserratum	160,489	90,517	17,432	26,270	114/134	80 (7)	30 (7)	4 (4)	20	37.7
O. huadongense	160,489	90,517	17,432	26,270	114/134	80 (7)	30 (7)	4 (4)	20	37.7

Table 1. *Cont.*

Species	Size (bp)	LSC Length (bp)	SSC Length (bp)	IR Length (bp)	Number of Different Genes/Total Number of Genes	Number of Different Protein-Coding Genes (Duplicated in IR)	Number of Different tRNA Genes (Duplicated in IR)	Number of Different rRNA Genes (Duplicated in IR)	Number of Genes Duplicated in IR	GC Content (%)
O. maximowiczii	159,714	85,567	23,685	25231	114/134	80 (7)	30 (7)	4 (4)	20	37.7
O. muliense	156,054	85,484	17,684	26,443	114/134	80 (7)	30 (7)	4 (4)	20	37.4
O. scaberulum	157,810	85,540	21,822	25,224	114/134	80 (7)	30 (7)	4 (4)	20	37.6
O. sieboldii	156,550	86,959	17,525	26,033	114/134	80 (7)	30 (7)	4 (4)	20	37.6
P. davidii	155,533	84,741	17,101	26,845 (26,846)	114/134	80 (7)	30 (7)	4 (4)	20	37.5
P. vulgare	154,730	85,023	17,761	25,973	114/134	80 (7)	30 (7)	4 (4)	20	37.5

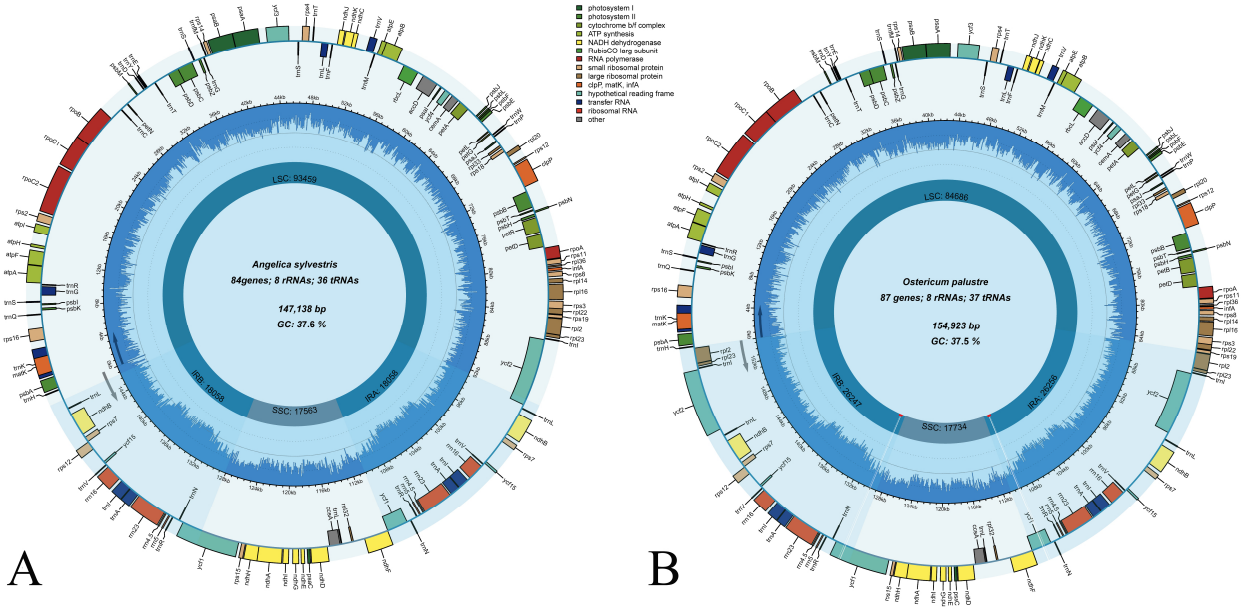

Figure 2. Plastid genome map of (**A**) *Angelica* and (**B**) *Ostericum* type-species. The species name and specific information regarding the genome (length, GC content, and the number of genes) are depicted in the center of the plot. The lengths of the corresponding single short copy (SSC), inverted repeat (IRa and IRb), and large single-copy (LSC) regions are shown. Represented with arrows, the transcription directions for the inner and outer genes are listed clockwise and anticlockwise, respectively. The optional shaded area stretching from the inner sphere toward the outer circle marks the IR regions. Genes are color-coded by their functional classification.

Table 2. List of genes and pseudogenes in *Angelica* and *Ostericum* species.

Category	Gene Group	Gene Name
Self-replication	Transfer RNA genes	*trnI-CAU* (*), *trnI-GAU* *, *trnL-UAA*, *trnL-CAA* *, *trnL-UAG*, *trnR-UCU*, *trnR-ACG* *, *trnA-UGC* *, *trnW-CCA*, *trnM-CAU*, *trnV-UAC*, *trnV-GAC* *, *trnF-GAA*, *trnT-UGU*, *trnT-GGU*, *trnP-UGG*, *trnfM-CAU*, *trnG-UCC*, *trnG-GCC*, *trnS-GGA*, *trnS-UGA*, *trnS-GCU*, *trnD-GUC*, *trnC-GCA*, *trnN-GUU* *, *trnE-UUC*, *trnY-GUA*, *trnQ-UUG*, *trnK-UUU*, *trnH-GUG*
	Ribosomal RNA genes	*rrn16* *, *rrn23* *, *rrn4.5* *, *rrn5* *
	RNA polymerase	*rpoA*, *rpoB*, *rpoC1*, *rpoC2*
	Small subunit of ribosome	*rps2*, *rps3*, *rps4*, *rps7* *, *rps8*, *rps11*, *rps12* *, *rps14*, *rps15*, *rps16*, *rps18*, *rps19* (*) (*rps19*, *ψrps19*)
	Large subunit of ribosomal proteins (LSU)	*rpl2* (*), *rpl14*, *rpl16*, *rpl20*, *rpl22*, *rpl23* (*), *rpl32*, *rpl33*, *rpl36*

Table 2. *Cont.*

Category	Gene Group	Gene Name
Genes for photosynthesis	Subunits of NADH-dehydrogenase	*ndhA*, *ndhB* *, *ndhC*, *ndhD*, *ndhE*, *ndhF*, *ndhG*, *ndhH*, *ndhI*, *ndhJ*, *ndhK*
	Subunits of photosystem I	*psaA*, *psaB*, *psaC*, *psaI*, *psaJ*
	Subunits of photosystem II	*psbA*, *psbB*, *psbC*, *psbD*, *psbE*, *psbF*, *psbH*, *psbI*, *psbJ*, *psbK*, *psbL*, *psbM*, *psbN*, *psbT*, *psbZ*
	Subunits of cytochrome	*petA*, *petB*, *petD*, *petG*, *petL*, *petN*
	Subunits of ATP synthase	*atpA*, *atpB*, *atpE*, *atpF*, *atpH*, *atpI*
	Large subunit of rubisco	*rbcL*
Other genes	Translational initiation factor	*infA*
	Protease	*clpP*
	Maturase	*matK*
	C-type cytochrome synthesis gene	*ccsA*
	Subunit of acetyl-CoA	*accD*
	Envelope membrane protein	*cemA*
	Conserved open reading frames (*ycf*)	*ycf1* * (*ycf1*, *ψycf1*), *ycf2* (*), *ycf3*, *ycf4*, *ψycf15* *
Total		*Angelica*: 129, *Ostericum*: 134

* Duplicated genes in both genera, (*) Duplicated genes only in *Ostericum*, *ψ* shows pseudogenes.

3.2. Analyses of Inverted Repeat Contraction and Expansion

To assess the expansion and contraction of the IR regions in *Angelica*, *Ostericum*, and *Pternopetalum* (which is related to *Ostericum* in the phylogenetic trees), we illustrated the junctions of IR/LSC and IR/SSC (Figure 3). The junctions between the single-copy regions and IR regions are designated as J_{LA} (LSC/IRA), J_{LB} (LSC/IRB), J_{SA} (SSC/IRA), and J_{SB} (SSC/IRB). Among all the species, the junctions of J_{SA} and J_{SB} exhibited high conservation in these three genera, but J_{LA} and J_{LB} exhibited significant differences between *Angelica* and *Ostericum*, which contrasted with J_{LA} and J_{LB} of *Ostericum* being the same as *Pternopetalum*. The positions of the junctions J_{SB} and J_{SA} are relatively consistent among genera: J_{SB} between the *ψycf1* gene and *ndhF* gene, and J_{SA} occurs in the *ycf1* gene. The specific description of the junctions among these genera are as follows.

In *Angelica*, junction J_{LB} occurs in the *ycf2* gene, with *ycf2* 435–669 bp located in the IRB region. Junction J_{LA} occurs between the *trnL-CAA* gene and *trnH-GUG* gene. The *trnL-CAA* gene located in the IRA region with 775–1009 bp away from J_{LA}, and the *trnH-GUG* gene located in the LSC region with 461–1042 bp away from J_{LA}. Junction J_{SB} is between the *ψycf1* gene and *ndhF* gene except for *A. dahurica*, in which J_{SB} occurs within the 69-bp end of the *ndhF* gene. Junction J_{SA} occurs in the *ycf1* gene, with 1609–1901 bp of the *ycf1* gene duplicated in the IRA region.

In *Ostericum*, the IR regions expand outwards by ~8000 bp such that the *ycf2*, *rpl23*, *rpl2*, and *trnI-CAU* genes are all contained within the IRs. Thus, junction J_{LB} occurs in the *rps19* gene, resulting in the duplication of part of this gene named *ψrps19* (81 bp) in the IRA region, and there is 3-bp noncoding sequence between J_{LA} and the *trnH-GUG* gene. Junction J_{SB} is between the *ψycf1* gene and *ndhF* gene, and there are 9–4906 bp of noncoding sequences between J_{SB} and the *ndhF* gene. Junction J_{SA} occurs in the *ycf1* gene, with 782–1939 bp of the *ycf1* gene duplicated in the IRA region.

In *Pternopetalum*, junctions J_{LA} and J_{LB} are completely consistent with *Ostericum*. In *P. davidii*, junction J_{SB} is between the *ψycf1* gene and *ndhF* gene, 87 bp of noncoding sequences away from J_{SB}, and junction J_{SA} occurs in *ycf1*, with 2399 bp of the *ycf1* gene duplicated in the IRA region. In *P. vulgare*, junction J_{SB} occurs within the 6-bp end of the

ndhF gene, and junction J_{SA} occurs in *ycf1*, with 1848 bp of the *ycf1* gene duplicated in the IRA region.

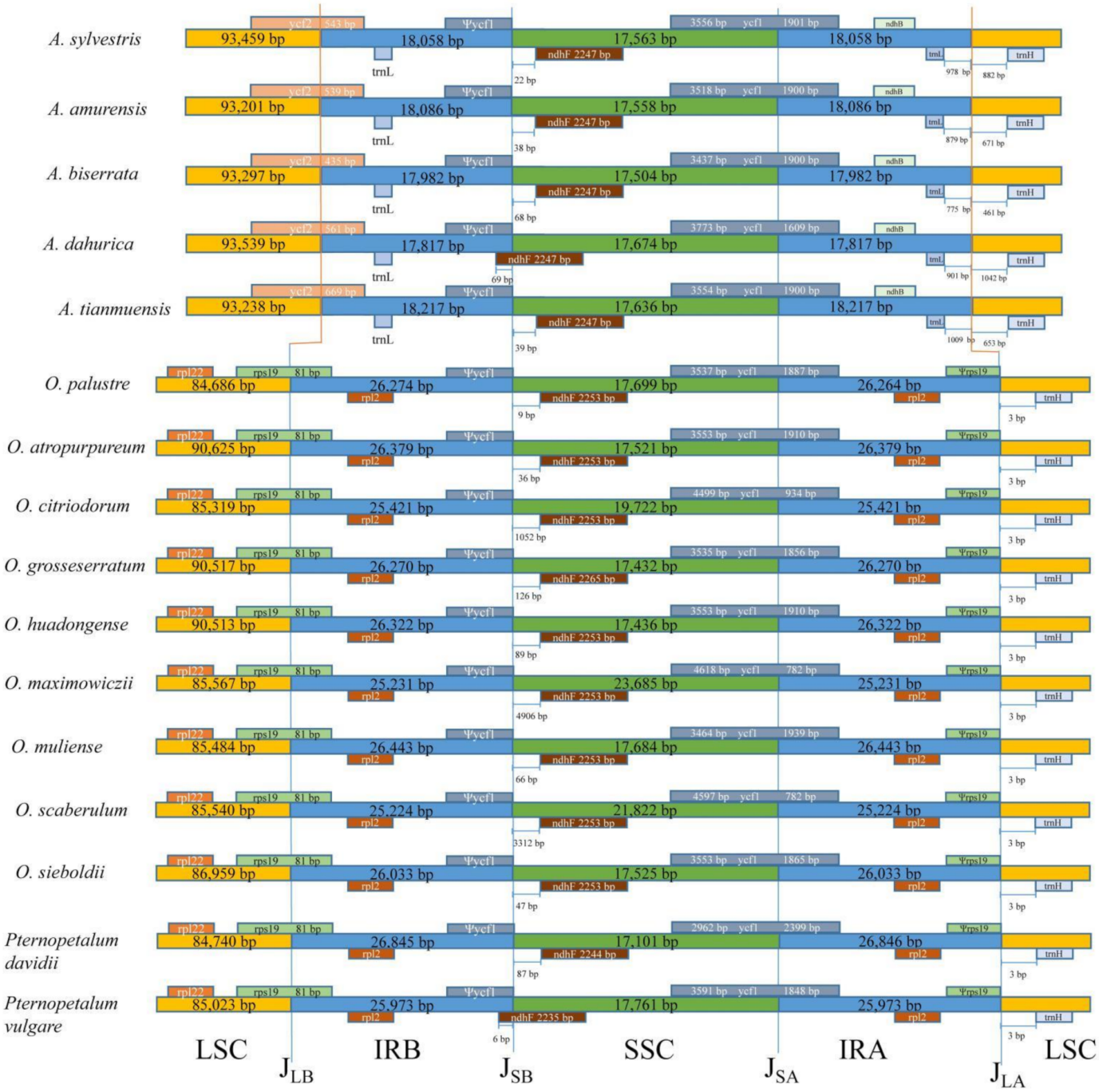

Figure 3. Comparison of the border regions *Angelica*, *Ostericum*, and *Pternopetalum* plastid genomes. LSC (large single-copy), SSC (small single-copy), and IR (inverted repeat) regions.

3.3. Single Sequence Repeat (SSR) Analyses

We detected six types of SSRs (mononucleotide, dinucleotide, trinucleotide, tetranucleotide, pentanucleotide, and hexanucleotide) in the *Angelica* and *Ostericum* plastomes (Figure 4). There was no discernible difference in the number of each SSR type, the total number of SSRs, and the distribution of SSRs in the plastomes between *Angelica* and *Ostericum* (Table S3, Figure S1). We identified 59–86 SSRs. In these species, *O. citriodorum* had the smallest number of SSRs (59) while *A. biserrate* had the largest (86). The number of

mononucleotide SSR was the largest, followed by dinucleotide, tetranucleotide, and trinucleotide repeats. Pentanucleotide and hexanucleotide repeats were very rare, especially hexanucleotide repeats (Figure 4). Most SSRs were located in the LSC region, followed by the SSC region, and then the IRA/IRB region (Figure S1). However, beyond this, we found that the repeat units of SSR types have similarities within the genus while appearing to be different between the two genera (Figure 4, Table S4).

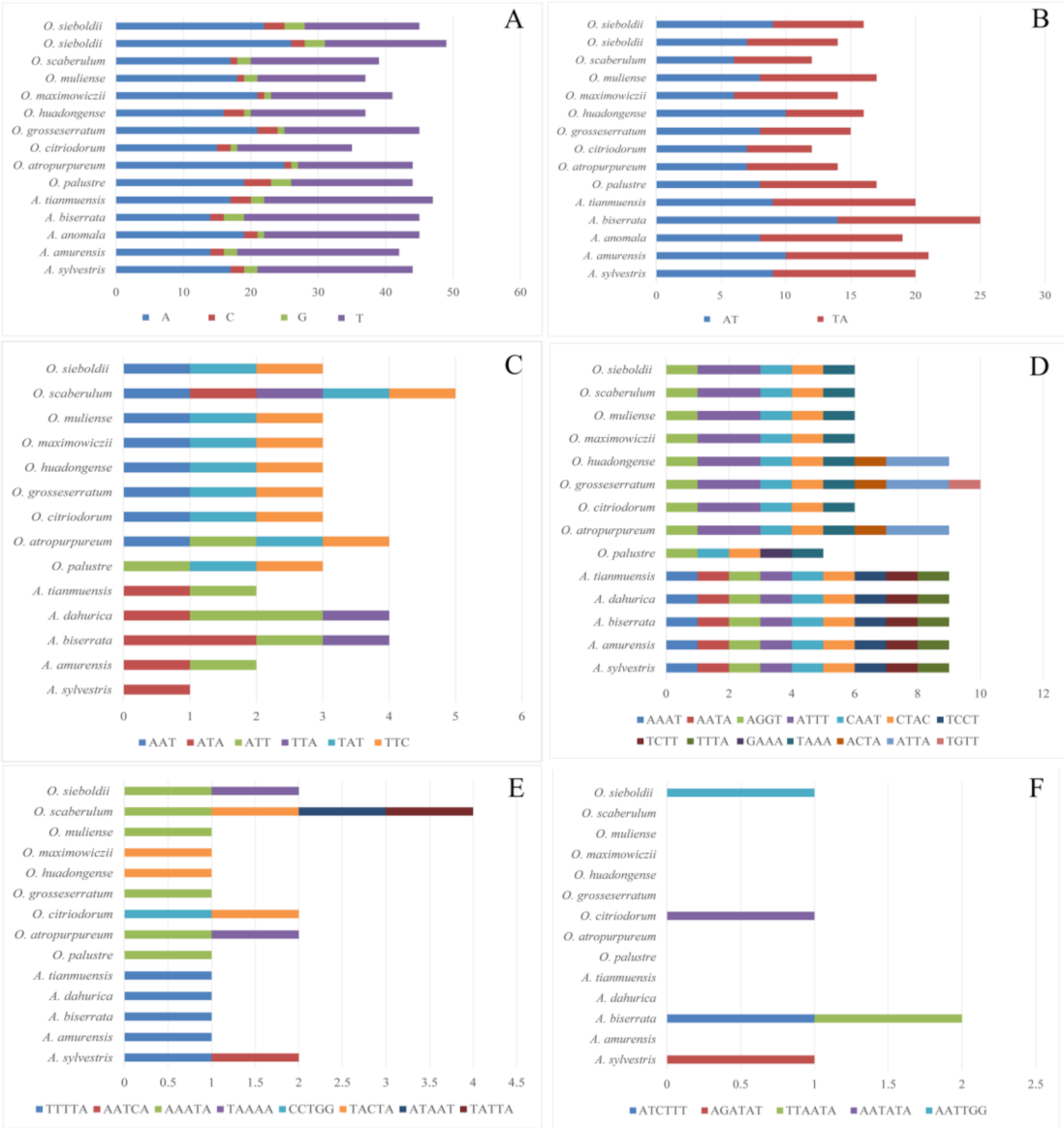

Figure 4. Repeat units of SSR types: (**A**) mononucleotide; (**B**) dinucleotide; (**C**) trinucleotide; (**D**) tetranucleotide; (**E**) pentanucleotide; and (**F**) hexanucleotide.

The type of SSR repeat unit was similar within the genus but different between *Angelica* and *Ostericum*, mainly showing trinucleotide, tetranucleotide, and pentanucleotide repeats (Figure 4C–E, Table S4). In the trinucleotide, the repeat units in *Angelica* were almost all ATT and ATA while in *Ostericum*, they were almost all TAT, AAT, and TTC. For the pentanucleotide repeat units, the *Angelica* species shared TTTTA, which was not detected in *Ostericum*, while most *Ostericum* species shared AAATA or TACTA, which were not detected in *Angelica*. The repeat units of tetranucleotides are special: AGGT, ATTT, CAAT, and CTAC were detected in both *Angelica* and *Ostericum*. However, the *Angelica* species shared TCCT, TCTT, TTTA, AAAT, and AATA within the genus and these repeat units were

not detected in *Ostericum*. On the other hand, the *Ostericum* species shared GAAA, TAAA, ACTA, and ATTA, which were not detected in *Angelica*.

3.4. Sequence Diversity Analyses

The mVISTA online program with the Shuffle-LAGAN mode was employed to analyze the comprehensive sequence discrepancy of *Angelica* and *Ostericum* using *P. vulgare* as a reference. The sequence identity results revealed that the whole plastome was conserved within the genus, but there were significant differences between *Angelica* and *Ostericum*. Plastomes among *Ostericum* and *Pternopetalum* were more similar and conservative (Figure 5). The IR regions were more conserved compared to the LSC and SSC regions and coding regions had more sequence conservation than noncoding regions for all genomes.

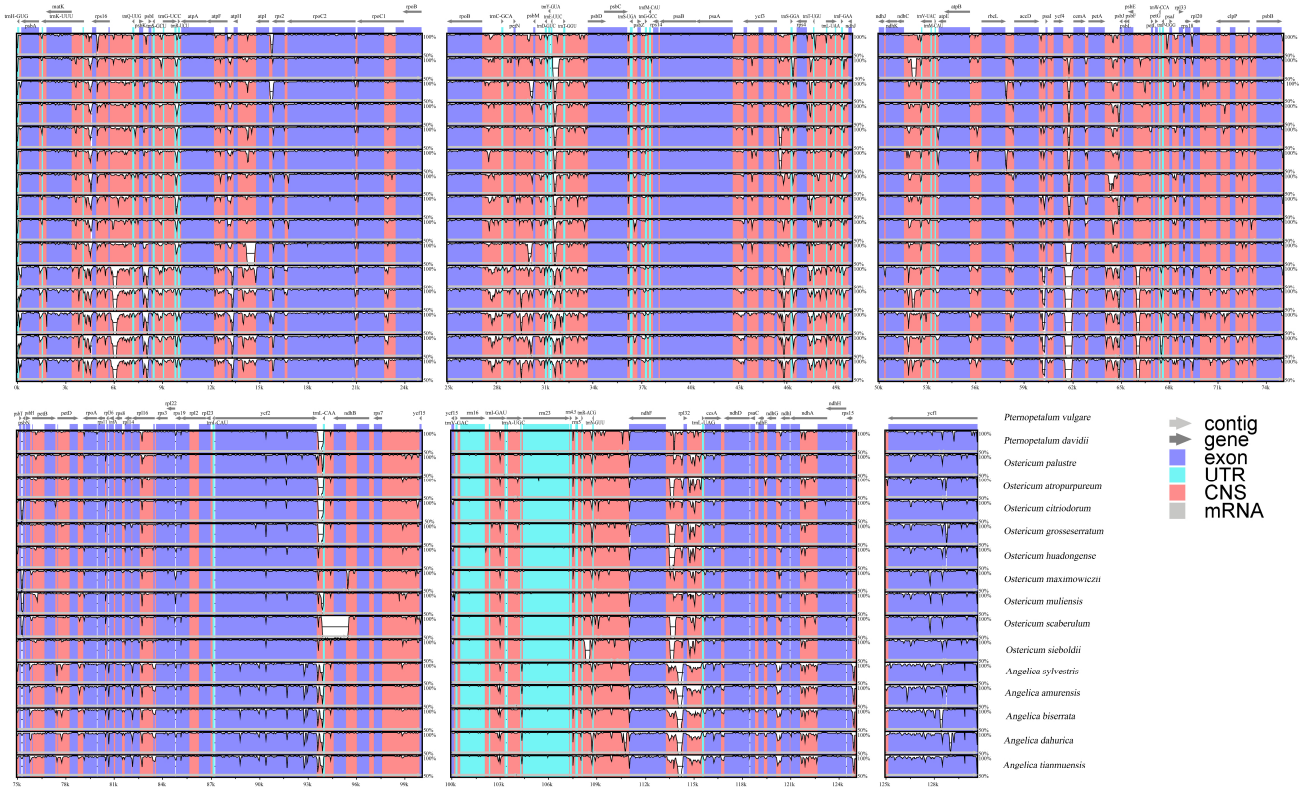

Figure 5. Sequence alignment of all the plastid genome sequences sequenced (*P. vulgare* as the reference). The y-axis represents the percent similarity between 50% and 100%. Different colors represent different genetic regions.

In addition, the nucleotide diversity (Pi) of plastomes in *Angelica* and *Ostericum* was calculated to estimate the sequence divergence level of different regions (Figure 6, Table S5). The nucleotide diversity results suggest that sequences with high Pi values are predominantly in intergenic spacers; however, the *ycf1* gene regions were an exception in both *Angelica* and *Ostericum*. In *Angelica* and *Ostericum*, the Pi values ranged from 0.00 to 0.025 and 0.00 to 0.23912, respectively. The corresponding averages of the *Angelica* and *Ostericum* plastome sequences were 0.0031 and 0.0059, respectively. We marked the regions with the top 10 Pi values in *Angelica* (Figure 6A). The top 10 Pi values are located in four regions, including the *trnE-UCC–trnT-GGU*, *petA–psbL*, *ndhF–rpl32*, and *ycf1* gene regions. Moreover, the *petA–psbL* region had the highest Pi values (0.025). In *Ostericum* (Figure 6B), the majority of the top 10 Pi values were located in *ψycf1–ndhF* and the highest Pi value was 0.23912. This difference is too large. This is because *O. maximowiczii* and *O. scaberulum* (Franch.) Yuan et Shan have longer sequences (~4000 bp) inserted between the *ycf1* pseudogene and *ndhF* gene. For comparison with *Angelica*, we chose another four

regions with high Pi values, excluding the *ψycf1–ndhF* region. The four regions were the *atpI–atpH*, *ndhC–trnV-UAC*, *psbH–petB*, and *ycf1* gene regions, respectively. Among them, the *psbH–petB* region had the highest Pi values (0.01894), excluding the *ψycf1–ndhF* region.

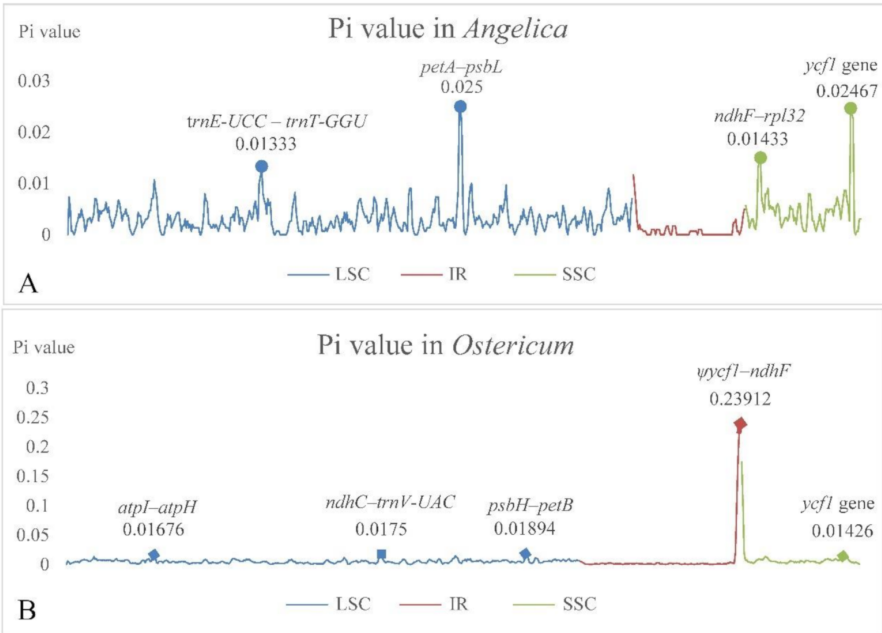

Figure 6. The nucleotide diversity of (**A**) five *Angelica* species and (**B**) nine *Ostericum* species. The regions with higher Pi values are marked. LSC (large single-copy), SSC (small single-copy), and IR (inverted repeat) regions.

3.5. Phylogenetic Analyses

To investigate the phylogenetic relationships between *Angelica* and *Ostericum*, we used 80 different protein-coding genes from 97 complete plastome sequences (14 newly sequenced in this study and 83 obtained from NCBI) to reconstruct phylogenetic trees based on the maximum likelihood (ML) and Bayesian inference (BI) methods (Figures 7 and S2). We also used 112 ITS sequences (we sequenced 5 sequences of *Angelica* and 17 sequences of *Ostericum*, listed in Table S2) to reconstruct phylogenetic trees between *Angelica* and *Ostericum* (Figures 7 and S3). The alignments of the CDS data sets for phylogenetic analysis showed a length of 62,264 bp, with 11,726 variable sites (18.83%) and 6525 parsimonyinformative characters (PICs; 10.48%). The alignments of the ITS data sets for phylogenetic analysis showed a length of 670 bp, with 411 variable sites (61.34%) and 357 parsimonyinformative characters (PICs; 53.28%).

Both the ML and BI analyses produced congruent tree topology, indicating that *Angelica* and *Ostericum* are not monophyletic. For *Angelica*, the majority of members are distributed in the Selineae tribe (plastid trees: BS = 100, PP = 1.00; ITS trees: BS = 60, PP = 0.72) while the rest (*A. ternate* Regel et Schmalh., *A. multicaulis* Pimenov, and *A. paeoniifolia* Shan et Yuan) are located in the *Hymenidium* (*Sinodielsia*) clade. However, *Ostericum* is located in the *Acronema* clade and is closely related to *Pternopetalum* (plastid trees: BS = 100, PP = 1.00; ITS trees: BS = 100, PP = 1.00). The relationships between *Ostericum* and *Angelica* were far from the phylogenetic trees. In addition, it is worth noting that *O. grosseserratum* (GenBank number: KT8524844) is a sister to *A. tianmuensis* (plastid trees: BS = 100, PP = 1.00) in the phylogenetic trees but the *O. grosseserratum* we sequenced in this study is located in *Ostericum* and is a sister to *O. atropurpureum* (plastid trees: BS = 100, PP = 1.00). In addition, *O. huadongense* was placed in *Ostericum* (plastid trees: BS = 100, PP = 1.00; ITS trees: BS = 100, PP = 1.00) rather than *Angelica* in this study. Thus, there is no doubt that *O. huadongense* is a member of *Ostericum*. *O. muliense* (R. H. Shan et F. T. Pu) Pimenov et Kljuykov clustered with the communities of *O. scaberulum* and *O. maximowiczii* (plastid

trees: BS = 100, PP = 1.00) or *O. muliense* is a sister to *O. scaberulum* (ITS trees: BS = 56, PP = 0.65). Furthermore, *Pterygopleurum neurophyllum* (Maxim.) Kitag. was inserted into *Ostericum* (plastid trees: BS = 100, PP = 1.00; ITS trees: BS = 100, PP = 1.00), leading to *Ostericum* not being monophyletic. In all tree topologies, *Ostericum* is a sister to *Pternopetalum* (plastid trees: BS = 1.00, PP = 100; ITS trees: BS = 0.52, PP = 61).

Figure 7. Phylogenetic relationships between *Angelica* and *Ostericum* and related groups are inferred from Bayesian inference (BI) based on the protein-coding genes of plastid genomes (**left**) and nrITS (**right**). Bayesian posterior probabilities (BI PPs) are presented at the nodes. The complete plastid genome sequences and ITS sequences obtained from NCBI show the GenBank number adjacent to the species names. *Angelica* is highlighted in blue, *Ostericum* is highlighted in red, and *Pternopetalum* is highlighted in green. The illustration of the fruit in the transverse section from top to bottom is *A. dahurica*, *O. scaberulum*, and *P. davidii*.

4. Discussion

4.1. Comparative Analyses of Plastomes

Generally, plastomes are highly conserved in genome structure, GC content, and gene order [60,61]. However, previous studies have confirmed that expansion and contraction of IRs in plastomes has often occurred in Apiaceae [62,63]. In this study, we conducted comparative analyses of these plastomes of *Angelica* and *Ostericum*, and all plastomes presented a typical quadripartite structure, including the LSC region, SSC region, and two IR regions. For all these plastomes, the SSC region contained the same 12 protein-coding genes (the protein-coding gene *ycf1* counted in the SSC region) and this is the same in Apioideae [37–39,64,65]. Moreover, the gene numbers distributed in the LSC and IR regions were different between *Angelica* and *Ostericum*. The LSC region had 64 protein-coding genes in *Angelica* while the LSC region had 61 protein-coding genes in *Ostericum*, and the IR region had 4 protein-coding genes in *Angelica* while the IR region had 7 protein-coding genes in *Ostericum*. However, the plastomes' characters of *Ostericum* were consistent with *Pternopetalum*. These results indicate that *Ostericum* is more similar to the genus *Pternopetalum* rather than the genus *Angelica* in genome structure, gene numbers, and gene order.

The contraction and expansion of IR regions is important for genome size variations [66–68]. The IRs of *Ostericum* and *Pternopetalum* were ~8000 bp longer than those of *Angelica*, causing the number of IR genes in *Ostericum* and *Pternopetalum* to be greater than that in *Angelica*. The expansion of IR regions in Apiaceae has been reported in previous studies, showing that junctions J_{SB} and J_{SA} have similar gene positions in all Apiaceae plastomes, and that IRs' expansion and contraction mainly occurred in J_{LA} and J_{LB} [43,62,63]. In this study, *Ostericum* was consistent with *Pternopetalum* in all junctions. However, in the junction of IR/LSC (J_{LA} and J_{LB}), contraction and expansion of IRs between *Angelica* and *Ostericum* was found. In addition, we observed that junctions J_{SA} and J_{SB} generated slight expansion and contraction. The IRB region expanded to the SSC region, as reflected in the junction J_{SB} with the *ndhF* gene in *A. dahurica* and *P. vulgare*, and this phenomenon appeared in *A. apaensis* [43]. Meanwhile, compared to other species in Apiaceae, the size of the SSC region, ranging from 17,436 to 23,685 bp in *Ostericum*, is unique [37,39,43,62,63,69]. The contraction and expansion of IRs suggests that *Ostericum* is more similar to the genus *Pternopetalum* rather than the genus *Angelica*.

Highly divergent regions were detected in plastomes, with Pi values indicating substitutions in the respective regions, and the highly divergent regions displayed high Pi values [38]. The mVISTA analyses and nucleotide diversity (Pi) results reveal that the IR regions were more conserved than the LSC and SSC regions [38,70,71]. Because intergenic regions are under weaker selection pressure and possess a higher evolutionary rate than genes, intergenic regions have more substitutions than gene regions [72,73]. Thus, intergenic regions are suitable for the study of the classification and evolution of low taxonomic levels, and plastid barcoding markers have been applied in some plants (e.g., *Salvia* subg. *Perovskia*) [72–74]. In this project, for *Angelica*, we found four regions with high Pi values (top 10 Pi values). For *Ostericum*, we also chose four regions with high Pi values, excluding the *ψycf1–ndhF* region. Among these regions, only the *ycf1* gene region was detected in both genera while the other regions did not overlap. Different highly divergent regions were selected for *Angelica* and *Ostericum*, which might be more suitable for the development of potential molecular markers and species identification for the two genera. Moreover, we observed that *Ostericum* had the highest Pi value and a higher average value, suggesting that *Ostericum* has more substitutions than *Angelica*. The different highly divergent regions observed in *Angelica* and *Ostericum* suggest that *Ostericum* may not be closely related to *Angelica*.

Due to the high level of polymorphism, simple sequence repeats (SSRs) have been recognized as one of the main sources of molecular markers and have been widely used in plant population genetics and evolutionary studies [34,75,76]. Furthermore, next-generation sequencing can be used to select SSRs and produce SSR markers more conveniently [77].

In our study, the most abundant SSRs were mononucleotides, followed by dinucleotide, tetranucleotide, trinucleotide, pentanucleotide, and hexanucleotide repeats (in decreasing abundance) in both genera. This result was common in *Allium* [78], Liliaceae [69], and Apiaceae [64]. The SSRs were mainly distributed in the LSC region, followed by the SSC region, and the same results have appeared in previous research studies [37,79]. The type of SSR repeat unit was similar within the genus but different between *Angelica* and *Ostericum*, mainly showing trinucleotide, tetranucleotide, and pentanucleotide sequences (Figure 4C–E, Table S4). Therefore, these SSRs may be promising SSR markers for the identification, classification, and genetic divergence of *Angelica* and *Ostericum*. The differences between SSR types indicated a distant relationship between *Angelica* and *Ostericum*.

4.2. Phylogenetic Position and Intergeneric Relationship of Ostericum

In the phylogenetic trees, our results exhibited significantly improved support and resolution. The relationships between *Angelica* and *Ostericum* established by 70 protein-coding genes were compatible with previous studies [8,15,16,80]. The species of *Angelica* were not grouped into a monophyletic group and the majority of members were distributed in the Selineae tribe while a few species were located in the *Hymenidium* (*Sinodielsia*) clade [8,81]. However, *Ostericum* occurred in the *Acronema* clade [8] and formed a monophyletic group with *P. neurophyllum* and *Ostericum* was found to be a sister to *Pternopetalum*. These phylogenetic studies confirm that *Ostericum* should be treated as an independent genus and that *Angelica* has a distant relationship with *Ostericum*.

Focusing on *Ostericum*, the sequence of *O. grosseserratum* obtained from GeneBank (GeneBank number: KT8524844) clustered with *A. tianmuensis* but that newly sequenced in this study occurred in *Ostericum*. From the genome size and molecular phylogenetic position, we found that KT8524844 has high consistency with *A. tianmuensis*. Thus, we consider that KT8524844 is probably the sequence of *A. tianmuensis*. In addition, *O. huadongense* occurred in *Angelica* and was found to be a sister to *Czernaevia laevigata* Turcz. in a previous study [16]. In our study, *O. huadongense* belonged to *Ostericum* and was found to be a sister to *O. sieboldii*. Therefore, *O. huadongense* is undoubtedly a member of *Ostericum*.

The position of the species *P. neurophyllum* is special, nested in the *Ostericum* clade and sister to *O. palustre*, the type-species of *Ostericum*. We examined the herbarium specimens of *P. neurophyllum* in iPlant (http://www.iplant.cn/; accessed on 28 May 2022) and found that *P. neurophyllum* is similar to *O. citriodorum* in morphology. These results imply that this species should be transferred into *Ostericum*. However, morphological data on *P. neurophyllum* is currently lacking, and further research is needed on *P. neurophyllum*. In addition, our phylogenetic analyses resolved the taxonomic controversy of *O. muliense*. *O. muliense* was first described by Yuan and Shan in 1985 as *O. maximowiczii* var. *alpinum* Yuan et Shan from Sichuan, SW China [82] and was accepted as *O. maximowiczii* var. *alpinum* in *Flora of China* [83]. However, Pimenov thought the taxon was a separate species in the combination of characters differing from *O. maximowiczii* by investigation of the type [17,20]. Our phylogenetic analyses uncovered that *O. scaberulum* is a sister to *O. maximowiczi* and then clustered with *O. muliense* in plastid trees. Though the phylogenetic position of *O. muliense* within *Ostericum* in ITS-based tree is uncertain (low BS and PP), this result still supports the conclusion of Pimenov that *O. muliense* is a separate species.

4.3. The Relationship between Angelica and Ostericum

Differences in the morphology and molecular phylogeny occurred in asexual fungal pathogen [84], phyllostomid bats [85], marsupials [86], *Hedyosmum* (Chloranthaceae) [4], Cannabaceae [87], *Phyllanthus* sensu lato (Phyllanthaceae) [88], Alangiaceae [89], *Acorus* (Acoraceae) [90], Restionaceae, Anarthriaceae, and Centrolepidaceae [5]. Traditional classifications of Apiaceae have relied almost exclusively on fruit characters such as fruit shape, the degree and direction of mericarp compression, modifications of the pericarp ribs (e.g., wings or spines), and the shape of mericarp commissural faces [7,11]. However, recent studies based on molecular phylogeny (based on ITS, ETS, and plastid DNA) do not agree

with the traditional classification of Apiaceae and revealed that most genera were not monophyletic (e.g., *Peucedanum* L. and *Ligusticum* L.) [7,8,65,91].

The taxonomic position of *Ostericum* is controversial in its taxonomic history. *Ostericum* has been treated as a member of *Angelica* [11,21]. Based on chemical studies, flavonoids are ubiquitous in *Ostericum* [23,92], and karyotypes and pollen ultrastructural studies suggest that *Ostericum* is a relatively independent genus from *Angelica* [25,26,93,94]. However, they still think that *Ostericum* is closely related to *Angelica* based on some similar morphological characteristics, especially fruit morphological characteristics (e.g., the lateral wings of mericarp are separate from each other, elliptic fruit, base slightly round or slightly heart-shaped, dorsally compressed, and vittae obvious) (Figures 1 and 7). On the contrary, the fruits of *Pternopetalum* are very different from the genus *Ostericum* (Figure 7) [9,10]. Though fruit anatomy and morphology suggested that *Ostericum* has convex and thickened outer walls and that the exocarp consists of one layer of cells, which is different from all other members of *Angelica* s.l. [16,24]. Combined with the conspicuous calyx teeth of *Ostericum* [9,10], we can only conclude that *Ostericum* is an independent genus from *Angelica*, and we still do not understand whether *Ostericum* is related to *Angelica*. However, our phylogenetic study revealed that *Ostericum* is closely related to *Pternopetalum* rather than *Angelica*, which contrasts with the fruit morphological features' distribution. This may be caused by convergent morphology and incomplete lineage sorting (ILS) [86,95–97]. Convergent morphology means that distinct lineages independently evolve similar morphological traits [97]. This may be the result of adaptation to shared environments. For *Ostericum* and *Angelica*, they share the same environment [9,10]. Convergence is widely used to interpret the phenomenon of morphological similarities between distantly related lineages. In addition, a recent study has shown that incomplete lineage sorting (ILS) makes ancestral genetic polymorphisms persist during rapid speciation events, and ILS is likely to have affected complex morphological traits in extant species [86]. Identification of the real reason for the phenomenon between *Angelica* and *Ostericum* requires more research.

5. Conclusions

In this study, we sequenced and annotated the plastomes of five species of *Angelica* and eight species of *Ostericum* (*O. sieboldii* with two populations). The plastome of *O. palustre* obtained from NCBI was added for analysis. We found that the plastomes of *Angelica* and *Ostericum* exhibited high conservation within the genus but presented significant differences between the two genera in genome size, gene numbers, IR junctions, nucleotide diversity, divergent regions, and the repeat units of SSR types. In contrast, *Ostericum* was more similar to *Pternopetalum* than *Angelica* in comparative analyses of the plastomes. These results of the plastome comparisons were consistent with the phylogenetic analyses. The phylogenetic analyses indicated that *Angelica* had a distant relationship with *Ostericum*: *Angelica* was mainly located in the Selineae tribe while *Ostericum* occurred in the *Acronema* clade and was found to be a sister to *Pternopetalum*. Our results robustly support the taxonomic treatment that separated *Ostericum* from *Angelica* as an independent genus and suggest that *Ostericum* is distantly related to *Angelica*. Furthermore, our results suggest that *O. muliense* is a separate species that differs from *O. maximowiczii* and imply that *P. neurophyllum* may be a member of *Ostericum*. There are differences in the comparative morphological analysis and molecular phylogeny between *Ostericum* and *Angelica*, and plastomes provide insights into these differences. The cause of the differences may be convergent morphology and incomplete lineage sorting (ILS). Our study provides abundant genetic resources for future molecular phylogeny, evolution, and population genetic studies of *Ostericum* and *Angelica*.

Supplementary Materials: The following supporting information can be downloaded at: https://www.mdpi.com/article/10.3390/d14090776/s1, Figure S1: Number of SSR types and SSRs' distribution; Figure S2: Phylogenetic relationships between *Angelica* and *Ostericum* and related groups are inferred from maximum likelihood (ML) based on the protein-coding genes of plastid genomes; Figure S3: Phylogenetic relationships between *Angelica* and *Ostericum* and related groups are inferred

from maximum likelihood (ML) based on nrITS; Table S1: Scientific names and abbreviations of the species; Table S2: Voucher details and GenBank accession numbers of taxa sequenced in this study; Table S3: Number of SSR types and SSRs' distribution; Table S4: Repeat units of SSR types; Table S5: Nucleotide diversity analyses of *Ostericum* and *Angelica*.

Author Contributions: Q.-P.J. and X.-J.H. conceived and designed the work. Q.-P.J. and D.-F.X. analyzed the sequence data. Q.-P.J. wrote the manuscript. C.-K.L., S.-D.Z. and X.-J.H. revised the manuscript. All authors have read and agreed to the published version of the manuscript.

Funding: This work was supported by the National Natural Science Foundation of China (Grant No. 32070221, 32170209, 31872647), National Herbarium of China, National Herbarium resources teaching specimen database (Grant No. 2020BBFK01), the Fundamental Research Funds for the Central Universities (2021SCU12097). The funding agencies had no role in the design of the experiment, analysis, and interpretation of data, and in writing the manuscript.

Institutional Review Board Statement: Not applicable.

Informed Consent Statement: Not applicable.

Data Availability Statement: The 14 annotated plastid sequences and 22 ITS sequences have been submitted to NCBI (https://www.ncbi.nlm.nih.gov) with accession numbers that can be found in Table S2.

Acknowledgments: We are grateful to the curators and staff of the Herbarium of Xinjiang Institute of Ecology and Geography Chinese Academy of Sciences (XJBI), the sample of *Angelica sylvestris* was taken from XJBI00022947.

Conflicts of Interest: The manuscript has not been published before and is not being considered for publication elsewhere. All authors declare there is no difference of interest.

Abbreviations

BI: Bayesian inference: bp: Base pair; BS: Branch support; PCGs: Protein-coding genes; CTAB: Cetyl trimethylammonium bromide; IR: Inverted repeat; ITS: Internal transcribed spacer; LSC: Large single copy; MCMC: Markov chain Monte Carlo; ML: Maximum Likelihood; NCBI: National Center for Biotechnology Information; PP: Posterior probability; rRNA: Ribosomal RNA; SSC: Small single copy; SSR: Simple sequence repeat; tRNA: Transfer RNA

References

1. Szöllősi, G.J.; Tannier, E.; Daubin, V.; Boussau, B. The Inference of Gene Trees with Species Trees. *Syst. Biol.* **2015**, *64*, e42–e62. [CrossRef] [PubMed]
2. The Angiosperm Phylogeny Group. An update of the Angiosperm Phylogeny Group classification for the orders and families of flowering plants: APG IV. *Bot. J. Linn. Soc.* **2016**, *181*, 1–20. [CrossRef]
3. The Angiosperm Phylogeny Group. An update of the Angiosperm Phylogeny Group classification for the orders and families of flowering plants: APG III. *Bot. J. Linn. Soc.* **2009**, *161*, 105–121. [CrossRef]
4. Zhang, Q.; Feild, T.S.; Antonelli, A. Assessing the impact of phylogenetic incongruence on taxonomy, floral evolution, biogeographical history, and phylogenetic diversity. *Am. J. Bot.* **2015**, *102*, 566–580. [CrossRef]
5. Briggs, B.G.; Marchant, A.D.; Perkins, A.J. Phylogeny of the restiid clade (Poales) and implications for the classification of Anarthriaceae, Centrolepidaceae and Australian Restionaceae. *Taxon* **2014**, *63*, 24–46. [CrossRef]
6. Downie, S.R.; Katz-Downie, D.S. A molecular phylogeny of Apiaceae subfamily Apioideae: Evience from nuclear ribosomal DNA internal transcribed spacer sequences. *Am. J. Bot.* **1996**, *83*, 234–251. [CrossRef]
7. Plunkett, G.M.; Downie, S.R. Major lineages within apiaceae subfamily apioideae: A comparison of chloroplast restriction site and dna sequence data. *Am. J. Bot.* **1999**, *86*, 1014–1026. [CrossRef]
8. Downie, S.R.; Spalik, K.; Katz-Downie, D.S.; Reduron, J.-P. Major clades within Apiaceae subfamily Apioideae as inferred by phylogenetic analysis of nrDNA ITS sequences. *Plant Divers. Evol.* **2010**, *128*, 111–136. [CrossRef]
9. Shan, R.H.; Sheh, M.L. Umbelliferae. In *Flora Reipublicae Popularis Sinicae*; Science Press: Beijing, China, 1992; Volume 55, p. 560.
10. Sheh, M.L.; Pu, F.T.; Pan, Z.H.; Watson, M.F.; Cannon, J.F.M.; Holmes-Smith, I.; Kljuykov, E.V.; Phillippe, L.R.; Pimenov, M.G. Apiaceae. In *Flora of China*; Wu, Z.-Y., Raven, P.H., Hong, D.-Y., Eds.; Science Press: Beijing, China; Missouri Botanical Garden Press: Saint Louis, MO, USA, 2005; Volume 14, pp. 1–205.
11. Drude, C.G.O. Umbelliferae. In *Die Natürlichen Pflanzenfamilien, Div.*; Engler, A., Prantl, K., Eds.; Wilhelm Engelmann: Leipzig, Germany, 1898; Volume 3, p. 187.

12. Zhou, J.; Peng, H.; Downie, S.R.; Liu, Z.W.; Gong, X. A molecular phylogeny of Chinese Apiaceae subfamily Apioideae inferred from nuclear ribosomal DNA internal transcribed spacer sequences. *Taxon* **2008**, *57*, 402–416.
13. Calviño, C.I.; Teruel, F.E.; Downie, S.R. The role of the Southern Hemisphere in the evolutionary history of Apiaceae, a mostly north temperate plant family. *J. Biogeogr.* **2016**, *43*, 398–409. [CrossRef]
14. Wen, J.; Yu, Y.; Xie, D.F.; Peng, C.; Liu, Q.; Zhou, S.D.; He, X.J. A transcriptome-based study on the phylogeny and evolution of the Taxonomically controversial subfamily Apioideae (Apiaceae). *Ann. Bot.* **2020**, *125*, 937–953. [CrossRef] [PubMed]
15. Feng, T.; Downie, S.R.; Yu, Y.; Zhang, X.; Chen, W.; He, X.; Liu, S. Molecular systematics of *Angelica* and allied genera (Apiaceae) from the Hengduan Mountains of China based on nrDNA ITS sequences: Phylogenetic affinities and biogeographic implications. *J. Plant Res.* **2009**, *122*, 403–414. [CrossRef] [PubMed]
16. Liao, C.; Downie, S.R.; Li, Q.; Yu, Y.; He, X.; Zhou, B. New Insights into the Phylogeny of *Angelica* and its Allies (Apiaceae) with Emphasis on East Asian Species, Inferred from nrDNA, cpDNA, and Morphological Evidence. *Syst. Bot.* **2013**, *38*, 266–281. [CrossRef]
17. Pimenov, M.G. Updated checklist of Chinese Umbelliferae: Nomenclature, synonymy, typification, distribution. *Turczaninowia* **2017**, *20*, 106–239. [CrossRef]
18. Pimenov, M.G. Updated checklist of Chinese Umbelliferae: Nomenclature, synonymy, typification, distribution. Supplementum. *Turczaninowia* **2018**, *21*, 113–123. [CrossRef]
19. Mathias, M.E.; Constance, L. *North American Flora*; The New York Botanical Garden Press: New York, NY, USA, 1944; Volume 28B.
20. Pimenov, M.G.; Kljuykov, E.V. Notes on some Sino-Himalayan species of Angelica and Ostericum (Umbelliferae). *Willdenowia* **2003**, *33*, 121–137. [CrossRef]
21. Maximowiz, C.J. *Angelica* sect. *Ostericum* Maxim. *Bull. Acad. Imp. Sci. Saint-Pétersbourg, sér.* **1874**, *3*, *19*, 249–276.
22. Kitagawa, M. *Ostericum* and *Angelica* from Manchurica and Korea(I). *J. Jpn. Bot.* **1935**, *12*, 229–246.
23. Harborne, J.B.; Heywood, V.H.; Chen, X.Y. Separation of *Ostericum* from *Angelica* on the basis of leaf and mericarp flavonoids. *Biochem. Syst. Ecol.* **1986**, *14*, 81–83. [CrossRef]
24. Qin, H.Z.; Li, B.Y.; Wu, Z.J.; Pan, Z.H. On the fruit anatomy of *Angelica* L. (s.l.) of East Asia and North America and its evolution. *Acta Bot. Boreali-Occident. Sin.* **1995**, *15*, 48–54.
25. Sheh, M.L.; Su, P.; Pan, Z.H. The comparative study of pollen morphology of *Angelica* L. between East Asia and North America. *J. Plant Resour. Environ.* **1997**, *6*, 41–47.
26. Shu, P.; Sheh, M.L. Ultrastructure of pollen exine in Peucedaneae Drude with reference to its systematic significance. *Acta Bot. Sin.* **2004**, *46*, 311–318.
27. Hiroe, M.; Constance, L. *Umbelliferae of Japan*; University of California Press: Berkeley, CA, USA, 1958; p. 39.
28. Downie, S.R.; Ramanath, S.; Katz-Downie, D.S.; Llanas, E. Molecular systematics of Apiaceae subfamily Apioideae: Phylogenetic analyses of nuclear ribosomal DNA internal transcribed spacer and plastid rpoC1 intron sequences. *Am. J. Bot.* **1998**, *85*, 563–591. [CrossRef]
29. Downie, S.R.; Katz-Downie, D.S.; Watson, M.F. A phylogeny of the flowing plant family Apiaceae based on chloroplast DNA rpl16 and rpoC1 intron sequences: Towards a suprageneric classification of subfamily Apioideae. *Am. J. Bot.* **2000**, *87*, 273–292. [CrossRef] [PubMed]
30. Downie, S.R.; Watson, M.F.; Spalik, K.; Katz-Downie, D.S. Molecular systematics of Old World Apioideae (Apiaceae): Relationships among some members of tribe Peucedaneae sensu lato, the placement of several island-endemic species, and resolution within the apioid superclade. *Can. J. Bot.* **2000**, *78*, 506–528.
31. Spalik, K.; Reduron, J.P.; Downie, S.R. The phylogenetic position of *Peucedanum* sensu lato and allied genera and their placement in tribe Selineae (Apiaceae, subfamily Apioideae). *Plant Syst. Evol.* **2004**, *243*, 189–210. [CrossRef]
32. Schneider, J.V.; Paule, J.; Jungcurt, T.; Cardoso, D.; Amorim, A.M.; Berberich, T.; Zizka, G. Resolving Recalcitrant Clades in the Pantropical Ochnaceae: Insights from Comparative Phylogenomics of Plastome and Nuclear Genomic Data Derived from Targeted Sequencing. *Front. Plant Sci.* **2021**, *12*, 638650. [CrossRef]
33. Asaf, S.; Khan, A.L.; Khan, A.R.; Waqas, M.; Kang, S.M.; Khan, M.A.; Lee, S.M.; Lee, I.J. Complete Chloroplast Genome of *Nicotiana otophora* and its Comparison with Related Species. *Front. Plant Sci.* **2016**, *7*, 843. [CrossRef]
34. Xie, D.F.; Yu, H.X.; Price, M.; Xie, C.; Deng, Y.Q.; Chen, J.P.; Yu, Y.; Zhou, S.D.; He, X.J. Phylogeny of Chinese *Allium* Species in Section *Daghestanica* and Adaptive Evolution of *Allium* (Amaryllidaceae, Allioideae) Species Revealed by the Chloroplast Complete Genome. *Front. Plant Sci.* **2019**, *10*, 460. [CrossRef]
35. Magallon, S.; Hilu, K.W.; Quandt, D. Land plant evolutionary timeline: Gene effects are secondary to fossil constraints in relaxed clock estimation of age and substitution rates. *Am. J. Bot.* **2013**, *100*, 556–573. [CrossRef]
36. Daniell, H.; Lin, C.S.; Yu, M.; Chang, W.J. Chloroplast genomes: Diversity, evolution, and applications in genetic engineering. *Genome Biol.* **2016**, *17*, 134. [CrossRef] [PubMed]
37. Guo, X.L.; Zheng, H.Y.; Price, M.; Zhou, S.D.; He, X.J. Phylogeny and Comparative Analysis of Chinese *Chamaesium* Species Revealed by the Complete Plastid Genome. *Plants* **2020**, *9*, 965. [CrossRef] [PubMed]
38. Li, J.; Xie, D.F.; Guo, X.L.; Zheng, Z.Y.; He, X.J.; Zhou, S.D. Comparative Analysis of the Complete Plastid Genome of Five *Bupleurum* Species and New Insights into DNA Barcoding and Phylogenetic Relationship. *Plants* **2020**, *9*, 543. [CrossRef]
39. Ren, T.; Li, Z.-X.; Xie, D.-F.; Gui, L.-J.; Peng, C.; Wen, J.; He, X.-J. Plastomes of eight *Ligusticum* species: Characterization, genome evolution, and phylogenetic relationships. *BMC Plant Biol.* **2020**, *20*, 519. [CrossRef]

40. Xie, D.F.; Yu, Y.; Deng, Y.Q.; Li, J.; Liu, H.Y.; Zhou, S.D.; He, X.J. Comparative Analysis of the Chloroplast Genomes of the Chinese Endemic Genus *Urophysa* and Their Contribution to Chloroplast Phylogeny and Adaptive Evolution. *Int. J. Mol. Sci.* **2018**, *19*, 1847. [CrossRef]
41. Liao, C.; Chen, X.; Chen, Y.; Gao, Y. The complete chloroplast genome of *Angelica sylvestris*, the type species of the genus Angelica (Apiaceae). *Mitochondrial DNA B Resour.* **2019**, *4*, 3596–3597. [CrossRef] [PubMed]
42. Liao, C.; Chen, X.; Tan, J.; Gao, Q. The complete chloroplast genome of *Ostericum palustre* (Apiaceae). *Mitochondrial DNA Part B* **2020**, *5*, 1357–1358. [CrossRef]
43. Wang, M.; Wang, X.; Sun, J.; Wang, Y.; Ge, Y.; Dong, W.; Yuan, Q.; Huang, L. Phylogenomic and evolutionary dynamics of inverted repeats across *Angelica* plastomes. *BMC Plant Biol.* **2021**, *21*, 26. [CrossRef]
44. Doyle, J.J. A rapid dna isolation procedure for small quantities of fresh leaf tissue. *Phytochem. Bull. Bot. Soc. Am.* **1987**, *19*, 11–15.
45. White, T.J.; Bruns, T.; Lee, S.; Taylor, J. Amplification and direct sequencing of fungal ribosomal RNA genes for phylogenetics. In *PCR Protocols: A Guide to Methods and Applications*; Academic Press: Cambridge, MA, USA, 1990; pp. 315–322. [CrossRef]
46. Dierckxsens, N.; Mardulyn, P.; Smits, G. NOVOPlasty: De novo assembly of organelle genomes from whole genome data. *Nucleic Acids Res.* **2017**, *45*, e18. [CrossRef]
47. Qu, X.J.; Moore, M.J.; Li, D.Z.; Yi, T.S. PGA: A software package for rapid, accurate, and flexible batch annotation of plastomes. *Plant Methods* **2019**, *15*, 50. [CrossRef] [PubMed]
48. Kearse, M.; Moir, R.; Wilson, A.; Stones-Havas, S.; Cheung, M.; Sturrock, S.; Buxton, S.; Cooper, A.; Markowitz, S.; Duran, C.; et al. Geneious Basic: An integrated and extendable desktop software platform for the organization and analysis of sequence data. *Bioinformatics* **2012**, *28*, 1647–1649. [CrossRef] [PubMed]
49. Zhang, D.; Gao, F.; Jakovlić, I.; Zou, H.; Zhang, J.; Li, W.X.; Wang, G.T. PhyloSuite: An integrated and scalable desktop platform for streamlined molecular sequence data management and evolutionary phylogenetics studies. *Mol. Ecol. Resour.* **2020**, *20*, 348–355. [CrossRef] [PubMed]
50. Zheng, S.; Poczai, P.; Hyvonen, J.; Tang, J.; Amiryousefi, A. Chloroplot: An Online Program for the Versatile Plotting of Organelle Genomes. *Front. Genet.* **2020**, *11*, 576124. [CrossRef] [PubMed]
51. Thiel, T.; Michalek, W.; Varshney, R.K.; Graner, A. Exploiting EST databases for the development and characterization of gene-derived SSR-markers in barley (*Hordeum vulgare* L.). *Theor. Appl. Genet.* **2003**, *106*, 411–422. [CrossRef] [PubMed]
52. Frazer, K.A.; Pachter, L.; Poliakov, A.; Rubin, E.M.; Dubchak, I. VISTA: Computational tools for comparative genomics. *Nucleic Acids Res.* **2004**, *32*, W273–W279. [CrossRef]
53. Librado, P.; Rozas, J. DnaSP v5: A software for comprehensive analysis of DNA polymorphism data. *Bioinformatics* **2009**, *25*, 1451–1452. [CrossRef]
54. Katoh, K.; Standley, D.M. MAFFT multiple sequence alignment software version 7: Improvements in performance and usability. *Mol. Biol. Evol.* **2013**, *30*, 772–780. [CrossRef]
55. Posada, D.; Crandall, K.A. MODELTEST: Testing the model of DNA substitution. *Bioinformatics* **1998**, *14*, 817–818. [CrossRef]
56. Stamatakis, A. RAxML version 8: A tool for phylogenetic analysis and post-analysis of large phylogenies. *Bioinformatics* **2014**, *30*, 1312–1313. [CrossRef]
57. Ronquist, F.; Teslenko, M.; Van der Mark, P.; Ayres, D.L.; Darling, A.; Hohna, S.; Larget, B.; Liu, L.; Suchard, M.A.; Huelsenbeck, J.P. MrBayes 3.2: Efficient Bayesian phylogenetic inference and model choice across a large model space. *Syst. Biol.* **2012**, *61*, 539–542. [CrossRef] [PubMed]
58. Letunic, I.; Bork, P. Interactive Tree Of Life (iTOL) v5: An online tool for phylogenetic tree display and annotation. *Nucleic Acids Res.* **2021**, *49*, W293–W296. [CrossRef] [PubMed]
59. Tamura, K.; Stecher, G.; Peterson, D.; Filipski, A.; Kumar, S. MEGA6: Molecular Evolutionary Genetics Analysis version 6.0. *Mol. Biol. Evol.* **2013**, *30*, 2725–2729. [CrossRef] [PubMed]
60. Bock, R.; Knoop, V. *Genomics of Chloroplasts and Mitochondria: Plastid Genomes of Seed Plants*; Springer: Berlin/Heidelberg, Germany, 2012; Volume 35, p. 23.
61. Wicke, S.; Schneeweiss, G.M.; DePamphilis, C.W.; Muller, K.F.; Quandt, D. The evolution of the plastid chromosome in land plants: Gene content, gene order, gene function. *Plant Mol. Biol.* **2011**, *76*, 273–297. [CrossRef] [PubMed]
62. Downie, S.R.; Jansen, R.K. A Comparative Analysis of Whole Plastid Genomes from the Apiales: Expansion and Contraction of the Inverted Repeat, Mitochondrial to Plastid Transfer of DNA, and Identification of Highly Divergent Noncoding Regions. *Syst. Bot.* **2015**, *40*, 336–351. [CrossRef]
63. Wen, J.; Xie, D.F.; Price, M.; Ren, T.; Deng, Y.Q.; Gui, L.J.; Guo, X.L.; He, X.J. Backbone phylogeny and evolution of Apioideae (Apiaceae): New insights from phylogenomic analyses of plastome data. *Mol. Phylogenet. Evol.* **2021**, *161*, 107183. [CrossRef]
64. Gou, W.; Jia, S.B.; Price, M.; Guo, X.L.; Zhou, S.D.; He, X.J. Complete Plastid Genome Sequencing of Eight Species from *Hansenia*, *Haplosphaera* and *Sinodielsia* (Apiaceae): Comparative Analyses and Phylogenetic Implications. *Plants* **2020**, *9*, 1523. [CrossRef]
65. Liu, C.K.; Lei, J.Q.; Jiang, Q.P.; Zhou, S.D.; He, X.J. The complete plastomes of seven *Peucedanum* plants: Comparative and phylogenetic analyses for the *Peucedanum* genus. *BMC Plant Biol.* **2022**, *22*, 101. [CrossRef]
66. Martin, W.; Deusch, O.; Stawski, N.; Grunheit, N.; Goremykin, V. Chloroplast genome phylogenetics: Why we need independent approaches to plant molecular evolution. *Trends Plant Sci.* **2005**, *10*, 203–209. [CrossRef]

67. Raubeson, L.A.; Peery, R.; Chumley, T.W.; Dziubek, C.; Fourcade, H.M.; Boore, J.L.; Jansen, R.K. Comparative chloroplast genomics: Analyses including new sequences from the angiosperms *Nuphar advena* and *Ranunculus macranthus*. *BMC Genom.* **2007**, *8*, 174. [CrossRef]
68. Yi, X.; Gao, L.; Wang, B.; Su, Y.J.; Wang, T. The complete chloroplast genome sequence of *Cephalotaxus oliveri* (Cephalotaxaceae): Evolutionary comparison of cephalotaxus chloroplast DNAs and insights into the loss of inverted repeat copies in gymnosperms. *Genome Biol. Evol.* **2013**, *5*, 688–698. [CrossRef] [PubMed]
69. Zhao, Z.; Liu, J.; Zhou, M.; Pan, Y. Chloroplast genome characterization of *Bupleurum dracaenoides*, a critically endangered woody species endemic to China, with insights of Apioideae phylogeny. *Gene Rep.* **2020**, *20*, 100784. [CrossRef]
70. Li, J.; Price, M.; Su, D.M.; Zhang, Z.; Yu, Y.; Xie, D.F.; Zhou, S.D.; He, X.J.; Gao, X.F. Phylogeny and Comparative Analysis for the Plastid Genomes of Five *Tulipa* (Liliaceae). *Biomed Res. Int.* **2021**, *2021*, 6648429. [CrossRef] [PubMed]
71. Xie, D.F.; Tan, J.B.; Yu, Y.; Gui, L.J.; Su, D.M.; Zhou, S.D.; He, X.J. Insights into phylogeny, age and evolution of *Allium* (Amaryllidaceae) based on the whole plastome sequences. *Ann. Bot.* **2020**, *125*, 1039–1055. [CrossRef] [PubMed]
72. Dong, W.; Liu, J.; Yu, J.; Wang, L.; Zhou, S. Highly variable chloroplast markers for evaluating plant phylogeny at low Taxonomic levels and for DNA barcoding. *PLoS ONE* **2012**, *7*, e35071. [CrossRef]
73. Hu, Y.; Woeste, K.E.; Zhao, P. Completion of the Chloroplast Genomes of Five Chinese *Juglans* and Their Contribution to Chloroplast Phylogeny. *Front. Plant Sci.* **2016**, *7*, 1955. [CrossRef] [PubMed]
74. Bielecka, M.; Pencakowski, B.; Stafiniak, M.; Jakubowski, K.; Rahimmalek, M.; Gharibi, S.; Matkowski, A.; Slusarczyk, S. Metabolomics and DNA-Based Authentication of Two Traditional Asian Medicinal and Aromatic Species of *Salvia* subg. *Perovskia*. *Cells* **2021**, *10*, 112. [CrossRef]
75. Powell, W.; Morgante, M.; Mcdevitt, R.; Vendramin, G.G.; Rafalski, J.A. Polymorphic simple sequence repeat regions in chloroplast genomes: Applications to the population genetics of pines. *Proc. Natl. Acad. Sci. USA* **1995**, *92*, 7759–7763. [CrossRef]
76. Gil, J.; Um, Y.; Kim, S.; Kim, O.T.; Koo, S.C.; Reddy, C.S.; Kim, S.C.; Hong, C.P.; Park, S.G.; Kim, H.B.; et al. Development of Genome-Wide SSR Markers from *Angelica gigas* Nakai Using Next Generation Sequencing. *Genes* **2017**, *8*, 238. [CrossRef]
77. Zalapa, J.E.; Cuevas, H.; Zhu, H.; Steffan, S.; Senalik, D.; Zeldin, E.; McCown, B.; Harbut, R.; Simon, P. Using next-generation sequencing approaches to isolate simple sequence repeat (SSR) loci in the plant sciences. *Am. J. Bot.* **2012**, *99*, 193–208. [CrossRef]
78. Xie, F.M.; Xie, D.F.; Xie, C.; Yu, Y.; Zhou, S.D.; He, X.J. Adaptation Evolution and Phylogenetic Analyses of Species in Chinese *Allium* Section *Pallasia* and Related Species Based on Complete Chloroplast Genome Sequences. *Biomed Res. Int.* **2020**, *2020*, 8542797. [CrossRef] [PubMed]
79. Yang, X.; Xie, D.F.; Chen, J.P.; Zhou, S.D.; Yu, Y.; He, X.J. Comparative Analysis of the Complete Chloroplast Genomes in *Allium* Subgenus *Cyathophora* (Amaryllidaceae): Phylogenetic Relationship and Adaptive Evolution. *Biomed. Res. Int.* **2020**, *2020*, 1732586. [CrossRef] [PubMed]
80. Liao, C.-Y.; Downie, S.R.; Yu, Y.; He, X.-J. Historical biogeography of the *Angelica* group (Apiaceae tribe Selineae) inferred from analyses of nrDNA and cpDNA sequences. *J. Syst. Evol.* **2012**, *50*, 206–217. [CrossRef]
81. Gou, W.; Guo, X.L.; Zhou, S.D.; He, X.J. Phylogeny and Taxonomy of *Meeboldia*, *Sinodielsia* and their relatives (Apiaceae: Apioideae) inferred from nrDNA ITS, plastid DNA intron (rpl16 and rps16) sequences and morphological characters. *Phytotaxa* **2021**, *482*, 121–142. [CrossRef]
82. Yuan, C.Q.; Shan, R.H. On the genera *Angelica* L. and *Ostericum* Hoffm. (Umbelliferae) in China. *Bull. Nanjing Bot. Gard.* **1985**, *1984–1985*, 1–5.
83. Pan, Z.H.; Waston, M.F. *Ostericum* Hoffm. In *Flora of China*; Wu, Z.Y., Raven, R.H., Eds.; Science Press: Beijing, China; Missouri Botanical Garden Press: Saint Louis, MO, USA, 2005; Volume 14, p. 3.
84. Stewart, J.E.; Timmer, L.W.; Lawrence, C.B.; Pryor, B.M.; Peever, T.L. Discord between morphological and phylogenetic species boundaries: Incomplete lineage sorting and recombination results in fuzzy species boundaries in an asexual fungal pathogen. *BMC Evol. Biol.* **2014**, *14*, 38. [CrossRef] [PubMed]
85. Davalos, L.M.; Cirranello, A.L.; Geisler, J.H.; Simmons, N.B. Understanding phylogenetic incongruence: Lessons from phyllostomid bats. *Biol. Rev. Camb. Philos. Soc.* **2012**, *87*, 991–1024. [CrossRef]
86. Feng, S.; Bai, M.; Rivas-Gonzalez, I.; Li, C.; Liu, S.; Tong, Y.; Yang, H.; Chen, G.; Xie, D.; Sears, K.E.; et al. Incomplete lineage sorting and phenotypic evolution in marsupials. *Cell* **2022**, *185*, 1646–1660. [CrossRef]
87. Yang, M.-Q.; Van Velzen, R.; Bakker, F.T.; Sattarian, A.; Li, D.-Z.; Yi, T.S. Molecular phylogenetics and character evolution of Cannabaceae. *Taxon* **2013**, *62*, 473–485. [CrossRef]
88. Bouman, R.W.; Keßler, P.J.A.; Telford, I.R.H.; Bruhl, J.J.; Strijk, J.S.; Saunders, R.M.K.; Welzen, P.C. Molecular phylogenetics of *Phyllanthus* sensu lato (Phyllanthaceae): Towards coherent monophyletic taxa. *Taxon* **2020**, *70*, 72–98. [CrossRef]
89. Feng, C.M.; Manchester, S.R.; Xiang, Q.Y. Phylogeny and biogeography of Alangiaceae (Cornales) inferred from DNA sequences, morphology, and fossils. *Mol. Phylogenet. Evol.* **2009**, *51*, 201–214. [CrossRef]
90. Chase, M.W. Monocot Relationships: An Overview. *Am. J. Bot.* **2004**, *91*, 1645–1655. [CrossRef]
91. Ren, T.; Xie, D.; Peng, C.; Gui, L.; Price, M.; Zhou, S.; He, X. Molecular evolution and phylogenetic relationships of *Ligusticum* (Apiaceae) inferred from the whole plastome sequences. *BMC Ecol. Evol.* **2022**, *22*, 55. [CrossRef]
92. Akbarian, A.; Rahimmalek, M.; Sabzalian, M.R.; Hodaei, M. Sequencing and phylogenetic analysis of phenylalanine ammonia lyase (pal) and chalcone synthase (chs) genes in some Iranian endemic species of Apiaceae. *Gene Rep.* **2021**, *23*, 101147. [CrossRef]

93. Pan, Z.H.; Zhuang, T.D.; Yao, X.M.; Sheng, N. A study on karyotypes and geographical distribution of *Angelica* and related genera (Umbelliferae) in China. *Acta Phytotax. Sin.* **1994**, *32*, 419–424.
94. Pan, Z.H.; Liu, X.T.; Li, X.H.; Yao, X.M.; Zhuang, T.D.; Lin, X. A Study on Karyotypes and Geographical Distribution of *Ostericum* (Umbelliferae) in China. *Acta Phytotax. Sin.* **1997**, *35*, 511–520.
95. Degnan, J.H.; Rosenberg, N.A. Gene tree discordance, phylogenetic inference and the multispecies coalescent. *Trends Ecol. Evol.* **2009**, *24*, 332–340. [CrossRef]
96. Cranston, K.A.; Hurwitz, B.; Ware, D.; Stein, L.; Wing, R.A. Species trees from highly incongruent gene trees in rice. *Syst. Biol.* **2009**, *58*, 489–500. [CrossRef]
97. Sackton, T.B.; Clark, N. Convergent evolution in the genomics era: New insights and directions. *Philos. Trans. R. Soc. Lond. B Biol. Sci.* **2019**, *374*, 20190102. [CrossRef]